Hydrol. Earth Syst. Sci. Discuss., doi:10.5194/hess-2016-344, 2016
Manuscript under review for journal Hydrol. Earth Syst. Sci.
Published: 15 July 2016

Hydrology and Earth System Sciences
Open Access
Discussions

Upscaling instantaneous to daily evapotranspiration using modelled daily shortwave radiation for remote sensing applications: an Artificial Neural Network approach

Loise Wandera[1,2], Kaniska Mallick[1], Gerard Kiely[3], Olivier Roupsard[4], Matthias Peichl[5], Vincenzo Magliulo[6]

[1]Remote Sensing and Ecohydrological Modeling, Dept. ERIN, Luxembourg Institute of Science and Technology, Belvaux, Luxembourg

[2]Water Resources, Dept. ITC, University of Twente, Enschede, Netherlands

[3]Hydrology, Micrometeorology & Climate Investigations, HYDROMET Research Group, University College Cork, Ireland

[4]CIRAD, UMR Eco & Sols, Montpellier, France

[5]Forest Landscape Biogeochemistry, Dept. Swedish University of Agricultural Sciences Umeå, Sweden

[6]Consiglio Nazionale delle Ricerche, ISAFOM, Ercolano (Napoli) - Italy

Correspondence to: Kaniska Mallick (Phone: +352 275888425; email: kaniska.mallick@gmail.com); Loise Wandera (email: loise.wandera@list.lu);

Hydrol. Earth Syst. Sci. Discuss., doi:10.5194/hess-2016-344, 2016
Manuscript under review for journal Hydrol. Earth Syst. Sci.
Published: 15 July 2016

Hydrology and Earth System Sciences
Discussions

Abstract

Upscaling instantaneous evapotranspiration retrieved at any specific time-of-daytime (ET_i) to daily evapotranspiration (ET_d) is a key challenge in regional scale vegetation water use mapping using polar orbiting sensors. Various studies have unanimously cited the short wave incoming radiation (R_S) to be the most robust reference variable explaining the ratio between ET_d and ET_i on the terrestrial surfaces. This study aims to contribute in ET_i upscaling for global studies using the ratio between daily and instantaneous incoming short wave radiation (R_{Sd}/R_{Si}) as a factor for converting ET_i to ET_d. The approach relies on the availability of R_{Sd} measurements that in many cases is hindered if not by cost but due to the environmental conditions such as cloudiness.

This paper proposes an artificial neural network (ANN) machine learning algorithm first to predict R_{Sd} from R_{Si} followed by using the R_{Sd}/R_{Si} ratio to convert ET_i to ET_d across different terrestrial ecosystem. Using R_{Si} and R_{Sd} observations from multiple subnetworks of FLUXNET database spread across different climates and biomes (to represent inputs that would typically be obtainable from remote sensors during the overpass time) in conjunction with some astronomical variables (derived from simple mathematical computation), we developed ANN model for reproducing R_{Sd} and further used it to upscale ET_i to ET_d. The efficiency of the ANN is evaluated for different morning and afternoon time-of-daytime, under varying sky conditions, and also at different geographic locations. Based on the measurements from 126 sites, we found R_S-based upscaled ET_d to produce a significant linear relation (R^2 = 0.65 to 0.69), low bias (-0.31 to -0.56 MJ m^{-2} d^{-1}) (appx. 4%), and good agreement (RMSE 1.55 to 1.86 MJ m^{-2} d^{-1}) (appx. 10%) with the observed ET_d, although a systematic overestimation of ET_d was also noted under persistent cloudy sky conditions. An intercomparison with existing upscaling method at daily, 8-day, monthly, and yearly temporal resolution revealed a robust performance of the ANN driven R_S method and was found to produce lowest RMSE under cloudy conditions. The overall methodology appears to be promising and has substantial potential for upscaling ET_i to ET_d for field and regional scale evapotranspiration mapping studies using polar orbiting satellites.

Key Words: Evapotranspiration, upscaling, short wave radiation, artificial neural networks, FLUXNET

Hydrol. Earth Syst. Sci. Discuss., doi:10.5194/hess-2016-344, 2016
Manuscript under review for journal Hydrol. Earth Syst. Sci.
Published: 15 July 2016

Hydrology and Earth System Sciences
Discussions

1 Introduction

Satellite-based mapping and monitoring of daily regional evapotranspiration (E_T hereafter) (or latent heat flux, λE) is considered as a key scientific concern for multitudes of applications including drought monitoring, water rights management, ecosystem water use efficiency assessment, distributed hydrological modelling, climate change studies, and numerical weather prediction (Anderson et al., 2015; Senay et al., 2015; Sepulcre-Canto et al., 2014). E_T variability during the course of a day is influenced by changes in the radiative energy being received at the surface (Brutsaert & Sugita, 1992; Crago, 1996; Parlange & Katul, 1992) and also due to soil moisture variability particularly in the water deficit landscapes. Therefore, one of the fundamental challenges in regional E_T modelling using polar orbiting sensors involves the upscaling of instantaneous E_T retrieved at any specific time-of-daytime (ET_i hereafter) to daily E_T (ET_d hereafter) For example, ET_i retrieved from LANDSAT, ASTER and MODIS sensors typically represent ET_i at single time snapshot of 1000, 1030 and 1330 local times, which needs to be upscaled to daily timescales for making this information usable to hydrologists and water managers (Cammalleri et al., 2014; Colaizzi et al., 2006; Ryu et al., 2012; Tang et al., 2013).

In order to accommodate the temporal scaling challenges encountered by remote sensing based E_T models, techniques have been proposed and applied by various researchers to upscale ET_i to ET_d. These include: (1) the constant evaporative fraction (EF) approach which assumes a constant ratio between λE and net available energy ($\phi = R_n - G$) during daytime [$EF = \lambda E/(R_n - G)$] (Gentine et al., 2007; Shuttleworth et al., 1989), (2) constant reference evaporative fractions (EF_r) where the ratio of ET_i between a reference crop (typically grass measuring a height of 0.12m in an environment that is not water limited) and an actual surface is assumed to be constant during daytime, allowing ET_d to be estimated from the daily EF_r (Allen et al.,1998; Tang et al., 2013), (3) constant global shortwave radiation method (R_S) where R_S is the reference variable at the land surface and it is assumed that the ratio of daily to instantaneous shortwave radiation (R_{Sd} and R_{Si}) values (i.e., R_{Sd}/R_{Si}) determines ET_d to ET_i ratio (Jackson et al., 1983; Cammalleri et al., 2014), and (4) constant extra-terrestrial radiation (R_STOA) where exo-atmospheric shortwave radiation (R_STOA) is the reference variable and the ratio of instantaneous to daily i.e. (R_{Si}TOA and R_{Sd}TOA) is assumed to determine the ratio of ET_d to ET_i (Ryu et al., 2012; Van Niel et al., 2012). These methods have been

Hydrol. Earth Syst. Sci. Discuss., doi:10.5194/hess-2016-344, 2016
Manuscript under review for journal Hydrol. Earth Syst. Sci.
Published: 15 July 2016

reviewed and compared in different studies with the view of identifying the most robust approach based on different data sets, time integrals and varying sky conditions (Cammalleri et al., 2014; Ryu et al., 2012; Tang et al, 2013, 2015; Van Niel et al., 2012; Xu et al., 2015).

Based on the previous studies, we find that the R_STOA approach performed consistently good at lower temporal resolution namely eight-day to monthly scales (Ryu et al., 2012; Van Niel et al., 2012) as well as under clear-sky conditions (Cammalleri et al., 2014), whereas the R_S approach was identified as the most preferred method for ET_i to ET_d conversion at a higher temporal scale i.e. daily timescale in addition to under variable sky conditions (Cammalleri et al., 2014; Chávez et el., 2008; Colaizzi, et al., 2006; Xu et al., 2015). Although the EF_r-based method produced comparable ET_d estimates as the R_S-based method, however the dependence of EF_r estimates on certain variables (e.g. daily ϕ and wind speed, which are difficult to characterise at the daily scale from single acquisition of polar orbiting satellites) (Tang et al., 2015) makes it a relatively less attractive method. Furthermore the EF-based method appeared to consistently underestimate ET_d in all these studies.

The motivation of the current work is built on the conclusions of Colaizzi et al. (2006), Chavez et al. (2008), Cammalleri et al. (2014), and Xu et al. (2015) that the ratio of the instantaneous to daily R_S incident on land surface is the most robust reference variable explaining the ratio between ET_d and ET_i among all the tested methods. In this work, we aim to contribute in ET_i upscaling by first developing a method for estimating R_{Sd} from any specific time-of-day R_S information (R_{Si}) and further using R_{Sd}/R_{Si} ratio as a factor for converting ET_i to ET_d. We develop an artificial neural network (ANN) machine learning algorithm (McCulloch & Pitts, 1943) in order to estimate R_{Sd}. ANN is an approach that has been successfully used in estimating global solar radiation in many sectors and more so in the field of renewable energy (Ahmad et al., 2015; Hasni et al., 2012; Lazzús et al., 2011). ANN is a non-linear model which works by initially understanding the behaviour of a system based on a combination of a given number of inputs and subsequently is able to simulate the system when fed with and independent set of inputs of the same system. Multi-layer perceptron (MLP) is one of the ANN architectures commonly used as opposed to other statistical methods, makes no prior assumptions concerning the data distribution, has ability to reasonably handle non-linear functions and reliably generalise independent data when presented (Gardner & Dorling, 1998; Khatib, Mohamed, & Sopian, 2012; Wang, 2003).

Hydrol. Earth Syst. Sci. Discuss., doi:10.5194/hess-2016-344, 2016
Manuscript under review for journal Hydrol. Earth Syst. Sci.
Published: 15 July 2016

Therefore the objectives of the present study are: (1) using a ANN with MLP architecture to predict R_{Sd}, (2) applying a method to upscale instantaneous ET_i to ET_d based on R_{Sd}/R_{Si} ratio under all sky conditions, and (3) comparing the proposed R_S-based method with R_STOA and EF-based E_T upscaling methods.

Even though this study is intended for remote sensing application, we tested the method using meteorological and heat fluxes measurements recorded in-situ by eddy covariance (EC) system at the FLUXNET (Baldocchi et al., 2001) sites mainly for the purpose of temporal consistency. However, we evaluate the performance in consideration with overpass time of polar orbiting satellites commonly used in E_T applications namely MODIS and LANDSAT. By choosing to use data distributed over different ecosystems and climates zones, we are faced with two problems : (1) changing cloud conditions across ecosystems, (2) varying Energy balance closure (EBC) requirements for the fluxes different ecosystems (Foken et al., 2006; Franssen et al., 2010; Mauder & Foken, 2006; Wilson et al., 2002). Cloudiness is a phenomenon that significantly influences the reliability of a model to predict incoming solar radiation as they are directly related to each other. Currently, information on cloudiness is obtainable from geostationary meteorological satellites, at hourly to 3-hourly time steps e.g. from the Clouds and Earth's Radiant Energy System (CERES), the International Satellite Cloud Climatology Project–Flux Data (ISCCP-FD), and Global Energy and Water cycle Experiment Surface Radiation Budget (GEWEX-SRB). The CERES algorithm uses cloud information from MODIS onboard both Terra and Aqua platforms and combines it with information from geostationary satellites to accurately capture the diurnal cycles of clouds. In this study, cloudiness is not included in the list of variables used to estimate R_{Sd} due to inconsistency in spatial resolution of data to match with the other predictive variables used. Including cloudiness holds a great potential in improving the ANN R_{Sd} predications due to their direct relationship. However, we assess the performance of the ANN under cloudy sky conditions based on simple cloudiness index computations as adopted from previous works (Baigorria et al., 2004). The EBC problems have been established to vary over landscapes due to management practices, climate, seasons and plant functional type characteristics (Foken et al., 2006). In this study, in order to test the robustness of the proposed method, we disregard the site specific EBC problems and assume that the systematic bias of fluxes fall within the same range across entire FLUXNET database used.

Hydrol. Earth Syst. Sci. Discuss., doi:10.5194/hess-2016-344, 2016
Manuscript under review for journal Hydrol. Earth Syst. Sci.
Published: 15 July 2016

Hydrology and Earth System Sciences
Discussions

2 Methodology

2.1 Rationale

The presented method of E_T upscaling from any specific time-of-daytime to daytime average evaporative fluxes is based on the assumption of self-preservation of incoming solar energy (i.e., shortwave radiation) as proposed by Jackson et al. (1983).

$$ET_d \approx ET_i \frac{R_{Sd}}{R_{Si}} \qquad (1)$$

Where, ET_d is the daytime average evapotranspiration in MJ m^{-2} d^{-1}, ET_i is the instantaneous evapotranspiration at any instance during daytime in W m^{-2}, R_{Si} and R_{Sd} are the values of shortwave radiation recorded at any instance and the daytime average having units W m^{-2} and MJ m^{-2} d^{-1}, respectively.

For any remote sensing studies using polar orbiting satellites, although the retrieval of ET_i and R_{Si} is has been carried (Tang et al., 2015; Huang et al., 2012; Laine et al., 1999; Polo et al., 2008), however estimating R_{Sd} and ET_d from R_{Si} and ET_i is still challenging. Presently, upscaling R_{Si} to R_{Sd} is primarily based on the clear sky assumption, i.e., for the entire daytime integration period, the sky remains cloud-free (Bisht et al., 2005; Jackson et al., 1983). However, the clear-sky assumption is not always appropriate for upscaling remote sensing based R_{Si} and hence ET_i because the sky conditions during a specific time-of-daytime may be clear whereas the other part of the day might be cloudy. Under such conditions, the clear-sky assumption of ET_i upscaling will lead to substantial overestimation of ET_d in cloudy conditions. Hence reliable estimates of all-sky (i.e., both clear and cloudy) R_{Sd} would greatly improve the ET_d estimates in the framework of Eq. (1). Given the unavailability of a definite method proposed to directly estimate all-sky R_{Sd} from R_{Si} information, here we have developed a simple method to upscale R_{Si} to R_{Sd} using ANN. This method uses the observations of both R_{Sd} and R_{Si} from all the available FLUXNET sites in conjunction with some ancillary variables to build the ANN as described below. A schematic diagram of the ANN method is given in Fig. 1.

Hydrol. Earth Syst. Sci. Discuss., doi:10.5194/hess-2016-344, 2016
Manuscript under review for journal Hydrol. Earth Syst. Sci.
Published: 15 July 2016

2.2 Development of Artificial Neural Network (ANN)

We used a multi-layer perceptron (MLP). The MLP was chosen as it has been widely used in many similar studies and cited to be a better alternative as compared to the conventional statistical methods (Ahmad et al., 2015; Chen et al., 2013; Dahmani et al., 2016; Mubiru & Banda, 2008). The MLP is composed of 5 neurons in the input layer, 1 output layer and 10 hidden layers (Fig. 2). The input layer neurons are made up of instantaneous incoming short wave radiation (R_{Si}), instantaneous exo-atmospheric shortwave radiation ($R_{Si}TOA$), daily exo-atmospheric shortwave radiation ($R_{Sd}TOA$), solar zenith angle (θ_Z), and day length (L_D) as the predictor variables whose values are initially standardized to range between -1 to 1. The choice of the inputs is intentionally limited to the variables that cannot only be acquired by measurements from meteorological stations but also derived from simple astronomical computations (Ryu et al., 2012)mainly to help minimize on the spatial distribution problem (as described earlier in the introduction) that is often linked to ground weather stations. In the MLP processing, the input layer directs the values of each input neuron x_i (i = 1, 2, 3…. n) unto each neuron (j) of the hidden layers. In the hidden layer x_i is multiplied by a weight (w_{ij}) and then a *bias* (b_j) assigned for each hidden layer also is applied. The weighted sum Eq. (2) is fed into a transfer function. In this work a tangent sigmoid (TANSIG) function is used Eq. (3) in the hidden layer while in the output layer a PURELIN function is applied Eq. (4) to give a single output value which is the predicted daily shortwave radiation (R_{Sd_pred}). The training of the ANN is completed by a regression analysis being performed internally by the algorithm between the target variable i.e. the observed and predicted daily shortwave radiation (R_{Sd_obs} and R_{Sd_pred}).

$$x_j = \int\left(\sum_{i=1}^{n} w_{ij} y_i b_j\right) \tag{2}$$

$$y_j = \frac{2}{\left(1+\exp\left(-2X_i\right)-1\right)} \tag{3}$$

$$y_j = X_i\left(PURELIN\right) \tag{4}$$

Bayesian regularization algorithm was chosen for the optimization process because it is able to handle noisy datasets by continuously applying adaptive weight minimization and can

Hydrol. Earth Syst. Sci. Discuss., doi:10.5194/hess-2016-344, 2016
Manuscript under review for journal Hydrol. Earth Syst. Sci.
Published: 15 July 2016

reduce or eliminate the need for lengthy cross-validation that often leads to overtraining and overfitting of models (Burden & Winkler, 2009).

2.3 Datasets

Daily and half-hourly data on R_S (W m^{-2}), R_{STOA}, net radiation (R_n, W m^{-2}), latent heat flux (λE, W m^{-2}), sensible heat flux (H, W m^{-2}) and ground heat flux (G, W m^{-2}) measured by the FLUXNET (Baldocchi et al., 2001) eddy covariance network were used. A total of 126 sites from the years 1999 to 2006 distributed between latitude 0-90 degrees north and south of the equator were used for the present analysis. The data sites covered a broad spectrum of vegetation functional types and climatic conditions and a list of the sites are given in Table S1 in the supplementary section.

Among the 126 sites, 85 sites were used for training and remaining 41 sites were used for validation. Partition of the data into training and validation was randomly selected regardless of the year. These translated into 194 and 86 yearly data for the respective sample. A global distribution of the data sites is shown in Fig. 3. From the training dataset, three samples were internally generated by the algorithm i.e., training datasets, validation datasets, and a testing dataset in a percentage ratio of 80:15:15 respectively. Considering the equatorial crossing time of different polar orbiting sensors like LANDSAT, ASTER, and MODIS Terra-Aqua, unique networks were generated for different time of day from morning to afternoon, and thus we had a total of 8 networks to represent potential satellite overpass times between 1030 to 1400 hours using 30 minutes interval as the closest reference time for each hour. The generated networks were then applied to an externally independent validation data set.

2.4 Intercomparison with other E_T upscaling methods

The performance of the R_S method is also compared with two other existing E_T upscaling methods: (a) the EF method (Cammalleri et al., 2014), where the reference variable is the net available energy (ϕ) (R_n - G).

$$SF_{EF} = \frac{\lambda E}{R_n - G} \tag{5}$$

$$ET_d = 1.1(R_n - G)SF_{EF}$$

Hydrol. Earth Syst. Sci. Discuss., doi:10.5194/hess-2016-344, 2016
Manuscript under review for journal Hydrol. Earth Syst. Sci.
Published: 15 July 2016

Where SF is the scaling factor, R_n is net radiation and G is ground heat flux.

(b) The exo-atmospheric irradiance method (Ryu et al., 2012) where the reference variable is R_STOA.

$$R_{Sd}TOA = S_{sc}\left[1 + 0.033cos\left(\frac{2\pi t_d}{365}\right)\right]cos\beta \quad (6)$$

$$SF_{RTOA} = \frac{R_{Sd}TOA}{R_{Si}TOA}$$

$$ET_d = ET_i SF_{RTOA}$$

Where S_{sc} is the solar constant (1360 W m^{-2}), t_d is the day of year, and β is computed solar zenith angle. We tested the performance of the three upscaling algorithms for all possible sky conditions assumed to be represented by daily atmospheric transmissivity (τ_d) (eq. 7) namely (i) 0.25≥τ≥0 (τ_1, hereafter), (ii) 0.5≥τ≥0.25 (τ_2, hereafter) (iii) 0.75≥τ≥0.5 (τ_3, hereafter), and (iv) 1≥τ≥0.75 (τ_4, hereafter), respectively. We use daily τ because it indicates the overall sky condition throughout a day.

$$\tau_d = \frac{R_{Sd}}{R_{Sd}TOA} \quad (7)$$

R_{Sd} and R_{Sd}TOA are daily shortwave radiation and the exo-atmospheric shortwave radiation in MJ m^{-2} d^{-1}.

2.5 Statistical error analysis

The relative performance of the ANN and three upscaling methods is evaluated using statistical indices generated namely: mean absolute percentage error (MAPE), root mean square error (RMSE), coefficient of determination (R^2), index of agreement (IA), and bias. ET_d estimates using the respective upscaling coefficients were compared with measured ET_d.

$$R^2 = 1 - \frac{\sum_{i=1}^{n}\left(p_i - o_i\right)^2}{\sum_{i=1}^{n}\left(o_i\right)^2} \quad (8)$$

Hydrol. Earth Syst. Sci. Discuss., doi:10.5194/hess-2016-344, 2016
Manuscript under review for journal Hydrol. Earth Syst. Sci.
Published: 15 July 2016

$$RMSE = \sqrt{\frac{\sum_{i=1}^{n}(o_i - p_i)^2}{n}} \quad (9)$$

$$MAPE = \frac{1}{n}\sum_{i=1}^{n}\frac{|o_i - p_i|}{n} * 100 \quad (10)$$

$$IA = \frac{\sum_{i}^{n}(p_i - o_i)^2}{\sum_{i=1}^{n}(|p_i - o_i| + |o_i - p_i|)^2} \quad (11)$$

$$Bias = \frac{\sum_{i=1}^{n}(p_i - o_i)}{n} \quad (12)$$

Where, n is the number of validation data; o_i and p_i are daily observed and estimated R_{Sd} or ET_d, respectively. $\bar{O}$ was the mean value of observed R_{Sd} or ET_d.

3 Results and discussion

3.1 Testing the performance of predicted R_{Sd}

Given that the performance of ET_d upscaling depends on the soundness of R_{Sd} estimation, we feel some justification to demonstrate the efficacy of the ANN method for predicting R_{Sd}. Figure 4 summarises the statistical results of predicted R_{Sd} (R_{Sd_pred}, hereafter) as obtained following the methodology described in the section 2.1, showing all the site-year average R^2, RMSE, IA, and MAPE values for eight different time-of-daytime upscaling slots. From the analysis it is apparent that the RMSE of R_{Sd_pred} from forenoon upscaling varied between 1.81-1.85 MJ m^{-2} d^{-1}, with MAPE, R^2, IA varying between 20–21%, 0.76–0.77, and 0.79 and 0.80, respectively (Fig. 4). For the afternoon, these statistics were almost similar and varied between 1.83–1.96 MJ m^{-2} d^{-1}, 19-20%, 0.75–0.77, and 0.80–0.81 (Fig. 4). Given the minimal discrepancy in error statistics from both forenoon and afternoon integration and considering the MODIS Terra-Aqua average overpass time we have considered 1100 and 1330 hours of daytime for the detailed follow up analysis.

Hydrol. Earth Syst. Sci. Discuss., doi:10.5194/hess-2016-344, 2016
Manuscript under review for journal Hydrol. Earth Syst. Sci.
Published: 15 July 2016

Figure 5 (a and b) shows the two dimensional scatters between R_{Sd_pred} versus R_{Sd_obs} for different levels of τ with an overall RMSE of 1.81 and 1.83 MJ m^{-2} d^{-1} for the forenoon and afternoon upscaling respectively. Table 1 and Fig. 5 clearly shows overestimation tendency of the current method under persistent cloudy sky conditions (τ_1), whereas the predictive capacity of the ANN model is reasonably strong with increasing atmospheric clearness. The RMSE of R_{Sd_pred} for different τ class from forenoon upscaling varied between 0.62 to 2.45 MJ m^{-2} d^{-1}, with MAPE, R^2 and IA of 9.2 to 53%, 0.67 to 0.98, and 0.67 to 0.95, respectively (Table 1). For the afternoon upscaling these statistics were 0.89 to 2.4 MJ m^{-2} d^{-1} (RMSE), 2.4 to 52% (MAPE), 0.65 to 0.98 (R^2), and 0.67 to 0.95 (IA) (Table 1).

The overestimation of R_{Sd_pred} at low values of τ is presumably associated with varying levels of cloudiness during the daytime. Since R_{Sd_pred} depends on the magnitude of R_{Si}, L_D, θ_Z, R_{SiTOA}, and R_{SdTOA}, there will be a tendency of overestimating R_{Sd_pred} on partly cloudy days if R_{Si} at a specific time-of-daytime is not affected by the clouds (L_D, θ_Z, R_{SiTOA}, and R_{SdTOA} are not influenced by the clouds).

3.2 Evaluation of predicted ET_d based on R_{Sd_pred}

Figure 6 summarises the statistical results of predicted ET_d (ET_{d_pred}, hereafter) using R_{Sd_pred}/R_{Si} as a scaling factor following eq. 1 for eight different time-of-daytime slots. Upon statistical evaluation, all the cases showed significantly linear relationship between ET_{d_pred} and observed ET_d(ET_{d_obs}, hereafter). The RMSE of ET_{d_pred} from forenoon upscaling varied from 1.67–1.84 MJ m^{-2} d^{-1}, with MAPE, R^2, IA varying between 30%–34%, 0.62–0.68, and 0.77–0.80, respectively (Fig. 6). For the afternoon upscaling, these statistics varied between 1.5–1.6 MJ m^{-2} d^{-1}, 29%–30%, 0.67–0.71, and 0.80 (Fig. 6). These results also indicate that the error statistics were nearly uniform and the accuracy of ET_{d_pred} varies only slightly when integration was done from different time-of-daytime hours between 1030 to 1400 h. These typical error characteristics can greatly benefit the ET_d modelling using polar orbiting data with varying overpass times between 1030 to 1400 hours. This also opens up the possibility to use either forenoon satellite (e.g., MODIS Terra, LANDSAT, ASTER etc.) or afternoon satellite (i.e., MODIS Aqua) to upscale ET_i to ET_d. Following R_{Sd}, here also we restricted our analysis to the two different time-of-daytime (1100h and 1330h) representing Terra and Aqua overpass times.

Hydrol. Earth Syst. Sci. Discuss., doi:10.5194/hess-2016-344, 2016
Manuscript under review for journal Hydrol. Earth Syst. Sci.
Published: 15 July 2016

Figure 7 (a and b) shows the two dimensional scatters between ET_{d_pred} versus ET_{d_obs} for different levels of daily τ with an overall RMSE, MAPE, and R^2 of 1.86 and 1.55 MJ m^{-2} d^{-1}, 31% and 36%, 0.65 and 0.69 for the forenoon and afternoon upscaling, respectively. As seen in Fig. 7, there is a systematic overestimation of ET_{d_pred} relative to the tower observed values under the low range of τ (i.e., cloudy sky). It is important to realise that, unlike ET_{d_obs}, ET_{d_pred} might be an outcome of ET_i instances when the sky was not overcast, i.e., the sky conditions might be clear at specific time-of-daytime but can be substantially overcast for the remainder of the daytime. As a result, any bias in the daily shortwave radiation prediction (R_{Sd_pred}) will result in biased ET_{d_pred} according to eq. 1, and the omission of non-clear sky conditions at any particular time of daytime would tend to lead to ET_{d_pred}>ET_{d_obs} for generally overcast days. Since ET_{d_obs} are the integrations of multiple ET_i measurements, such conditions could be conveniently captured in the observations which were not possible in the current framework of ET_{d_pred}. Therefore, when upscaling was done under clear skies at nominal acquisition time for generally overcast days, higher errors in ET_{d_pred} can be expected (Cammalleri et al., 2014). We examined this cloudy sky overestimation pattern in greater detail by evaluating the error statistics in ET_{d_pred} for four different levels of daily τ categories (Fig. 8).

The statistical evaluation of ET_{d_pred} for different classes of daily τ indicates the tendency of higher RMSE and low R^2 in ET_{d_pred} under the persistent cloudy-sky conditions (τ_1), while the performance of ET_{d_pred} is reasonably good with increasing atmospheric clearness (τ_2, τ_3, and τ_4) (Fig. 8). The RMSE of ET_{d_pred} for different τ class from forenoon upscaling varied between 1.09 to 2.96 MJ m^{-2} d^{-1}, with MAPE, R^2 and IA of 25 to 75%, 0.38 to 0.79, and 0.71 to 0.82, respectively. For the afternoon upscaling, these statistics were 0.98 to 2.02 MJ m^{-2} d^{-1} (RMSE), 24 to 87% (MAPE), 0.40 to 0.68 (R^2), and 0.71 to 0.77 (IA). Biome specific evaluation of ET_{d_pred} (Fig. 9) revealed lowest RMSE and highest R^2 both in the grassland (GRA) (0.68 to 1.14 MJ m^{-2} d^{-1}; 0.53 to 0.79) and shrubland (SH) (0.66 to 1.76 MJ m^{-2} d^{-1}; 0.60 to 0.82) whereas the RMSE was comparatively high over the tropical evergreen broadleaf forests (EBF) (1.41 to 2.02 MJ m^{-2} d^{-1}) and deciduous broadleaf forests (DBF) (1.94 to 2.55 MJ m^{-2} d^{-1}).

Hydrol. Earth Syst. Sci. Discuss., doi:10.5194/hess-2016-344, 2016
Manuscript under review for journal Hydrol. Earth Syst. Sci.
Published: 15 July 2016

Figure 10 shows the time series comparisons between observed ET_d and ET_{d_pred} for four different stations representing different latitude bands of both the Northern (Sweden) and Southern (Brazil, Australia, and South Africa) hemispheres. These reveal that the temporal dynamics of ET_d is in general consistently captured by the proposed method throughout year. In Br_SP1, relatively less seasonality was found in both observed and predicted ET_d. This is because SP1 is a tropical site having an annual rainfall of 850–1100 mm most of which is evenly distributed between March to end of September. The peaks in ET_d values during the beginning of year and October onwards coincided with the periods of increased R_S, and ET_{d_pred} could reasonably capture the observed trends during both rainy and non-rainy periods. Similarly the low ET_d pattern (10 to 50 W m^{-2}) (equivalent to 0.1 to 1 mm d^{-1}) in the hot arid climate of South Africa (Za-Kru) could also be reasonable captured in ETd_pred (Fig. 10). ET_{d_pred} over two other Southern hemisphere (AU-Tum) and the Northern hemisphere (SE-Fla) sites have shown distinct seasonality (high summer and low winter ET_d) coinciding with the observed ET_d patterns.

3.3 Comparison with existing ET upscaling methods

$ET_{d_}$pred from the proposed method was intercompared with two other upscaling schemes (R_STOA and EF) over the 41 FLUXNET validation sites for two different time-of-daytime, 1100h and 1330h, the statistics of which are given in Table 2. This comparison was also carried out according to different τ classes as defined in section 2.2.3.

From Table 2 it is apparent that the R_S-based method has generally produced relatively low RMSE (1.21 to 1.99 MJ m^{-2} d^{-1}) and MAPE (23 to 50%) as well as relatively high IA (0.72 to 0.84) as compared to the R_STOA and EF-based upscaling methods. The EF upscaling method appears to systematically underestimate ET_d for both forenoon and afternoon as evident from high negative bias compared to the other two methods (Table 2). On comparing R_S and R_STOA methods, the R_S-based method performed relatively better than the R_STOA scheme for the lower magnitude of τ classes. However, the results suggest comparable performance of R_STOA approach under clear sky conditions which are reflected in lowest RMSE (1.09 and 1.13 MJ m^{-2} d^{-1}) in ET_{d_pred} as compared to the other τ classes. In general, all the schemes performed relatively better from the afternoon upscaling as compared to the morning

Hydrol. Earth Syst. Sci. Discuss., doi:10.5194/hess-2016-344, 2016
Manuscript under review for journal Hydrol. Earth Syst. Sci.
Published: 15 July 2016

upscaling (as evidenced in higher R^2 and lower bias) (Table 2 and Fig. 8) which is in agreement with the findings from Ryu et al. (2012).

The tendency of positive bias in ET_{d_pred} from both R_S and R_STOA in clear skies from afternoon upscaling is partly explained by the fact that, during the afternoon the values of both R_S and R_STOA reached maximum limit and dominates their daily values (Jackson et al., 1983). The post afternoon rate of reduction in ET does not coincide with the shortwave radiation due to stomatal controls on ET, and the total water flux from morning to afternoon (0700h to 1300h) is generally greater than the total water flux from post afternoon (1500h onwards) till sunset. Therefore multiplying 1330h ET_i with high magnitude of R_{Sd}/R_{Si} or $R_{Sd}TOA/R_{Si}TOA$ would likely lead to an overestimation of ET_{d_pred} in the clear sky days.

Since extraterrestrial shortwave radiation is not affected by the clouds, ET_{d_pred} from R_STOA performed comparably with the R_S-based ET_{d_pred} with increasing atmospheric clearness (i.e., for the higher levels of daily τ). However, increased differences in the RMSE of ET_{d_pred} between R_S and R_STOA upscaling in the predominantly cloudy days indicates that more deviations can be expected in ET_{d_pred} from these two different method of upscaling under principally overcast conditions (Tang et al., 2013). This happens because the ratio of $R_{Sd}TOA/R_{Si}TOA$ is not impacted by the clouds and the magnitude of this ratio becomes markedly different from R_{Sd}/R_{Si} ratio in the presence of clouds, which leads to the differences in ET_{d_pred} between them. The R_S-based method is relatively efficient to discriminate the impacts on ET by R_{Sd}/R_{Si} due to the clouds. The generally good performance of R_S-based method and comparable error statistics with R_STOA-based ET_d estimates are consistent with the findings of Cammalleri et al. (2014) and Van Niel et al. (2012).

The systematic ET_d underestimation by EF method and nearly similar pattern of bias from two different time-of-daytime upscaling (Table 2) further points to the fact that the concave-up shape of the EF during daytime (Hoedjes et al., 2008; Tang et al., 2013) will tend to underestimate ET_d if EF is assumed to be conservative during the daytime. EF remains conservative during the daytime under extremely dry conditions when ET_d is solely driven by deep layer soil moisture. The systematic underestimation of ET_d from EF upscaling method corroborates with the results reported by other researchers (Cammalleri et al., 2014; Delogu et al., 2012; Gentine et al., 2007; Hoedjes et al., 2008) which suggests that the self-preservation

Hydrol. Earth Syst. Sci. Discuss., doi:10.5194/hess-2016-344, 2016
Manuscript under review for journal Hydrol. Earth Syst. Sci.
Published: 15 July 2016

of EF is not generally achieved, and this systematic underestimation of ET_d can be partially compensated if EF based ET upscaling is done from morning 0900h or afternoon 1600h time-of-daytime.

We further resampled ET_d (both predicted and observed) from daily to 8-day, monthly, and annual scale, and statistical metrics from the three different upscaling methods at three different temporal scales are shown in Fig. 11 and Table 3. Averaging ET_d over 8-day, monthly and annual scale substantially reduced the RMSE to the order of 60 to 70% for all the three upscaling methods. The R_S-based upscaled ET from morning and afternoon showed reduction in RMSE from 1.79 MJ to 0.57 MJ and 1.74 MJ to 0.51 MJ from daily to annual ET, respectively. For the other two upscaling method these statistics varied from 1.85 and 1.89 MJ to 0.62 and 0.53 MJ (R_STOA method), and 2.16 and 1.33 MJ to 2.20 and 1.31 MJ (EF method) (Fig. 11 and Table 3). The impact of daily cloud variability might have smoothed out in 8-day, monthly and annual scale which led to reduced RMSE and higher correlation between observed and predicted ET_d. Nearly the same error statistics in ET_{d_pred} from both the morning and afternoon upscaling also substantiates the findings of Ryu et al. (2012) and greatly stimulate the use of either morning satellite (i.e., Terra) or after satellite (i.e., Aqua) to upscale ET_i to ET_d or 8-day mean ET_d.

4 Summary and Conclusions

Given the significance of ET_d in remote sensing based water resource management from polar orbiting satellites, this study developed and evaluated a temporal upscaling method for estimating ET_d from different time-of-daytime instantaneous ET (ET_i) measurements with the assumption that the ratio between daytime to instantaneous R_S (R_{Sd}/R_{Si}) is the predominant factor governing ET_d/ET_i ratio. However, since R_{Sd} is not measurable from the polar orbiting satellites, we first developed a robust ANN based method to upscale R_{Si} to R_{Sd} followed by using the ratio of R_{Sd}/R_{Si} to further upscale ET_i to ET_d. The overarching goal of this study is to provide an operational and robust ET_i upscaling protocol for estimating ET_d from any polar orbiting satellite.

Based on the measurements from 126 flux tower sites, we found R_S-based upscaled ET_d to produce a significant linear relation (R^2 = 0.65 to 0.69), little bias (-0.31 to -0.56 MJ m^{-2} d^{-1}) (appx. 4%), and good agreement (RMSE 1.55 to 1.86 MJ m^{-2} d^{-1}) (appx. 10%) with the

Hydrol. Earth Syst. Sci. Discuss., doi:10.5194/hess-2016-344, 2016
Manuscript under review for journal Hydrol. Earth Syst. Sci.
Published: 15 July 2016

observed ET_d. While the R_STOA-based method appeared to produce slightly lower RMSE (10% lower) under cloud-free conditions (Table 2), R_S method demonstrates more robust performance and was found to be better under cloudy conditions. Despite the R_S method yielded relatively better overall accuracy in ET_{d_pred} statistics when compared with the R_STOA and EF-based method, statistical analysis of the ET_{d_pred} accuracy of the different temporal upscaling methods (as discussed in section 3.3) suggests that R_S and R_STOA to produce commensurate results under coarse temporal resolutions (Table 3). Therefore, at the coarse temporal scale (8-day and above), there was no preferred ET_i scaling method between R_S and R_STOA.

Among all the upscaling method tested, R_S–based method carries maximum information on the cloudiness and produced generally lowest RMSE, low bias (Table 3), and, therefore, overall the preferably robust scaling mechanism (at the daily scale) among all the other methods tested. However, upscaling large-area satellite-based ET_i by using retrieved R_{Si} would require accurate R_{Si} retrieval techniques, which are currently commonplace (Ahmad et al., 2015; Boulifa et al., 2015; Dahmani et al., 2016; Hasni et al., 2012; Li, Tang, Wu, & Liu, 2013) to support regional scale hydrological applications. Of the two other upscaling methods, R_STOA could be easily applied over large areas, had lower errors than EF, had second best RMSD, and overall lowest bias among the two. We conclude that using modelled R_S to upscale ET_i at daily scale appears to be viable for large-area hydrological remote sensing applications from polar orbiting satellites irrespective of any sky conditions.

The principal limitation of the approach is the dependence of ET_d and RS_d on single snapshot of ET_i and RS_i. Although hourly R_S data from geostationary satellite are becoming available; but these are available as sectorial products (i.e. for particular continents) instead of full global coverage. Ongoing efforts to develop geostationary based data by merging multiple geostationary satellites tend to overcome this limitation.

Acknowledgements

The authors thank HiWET (High resolution modelling and monitoring of water and energy transfers in WETland ecosystems) project funded through the Belgian Science Policy (BELSPO) and FNR under the programme STEREOIII (INTER/STEREOIII/13/03/HiWET). We thank entire FLUXNET site PIs for sharing the eddy covariance data. This work used

eddy covariance data acquired by the FLUXNET community and in particular by the following networks: AmeriFlux (U.S. Department of Energy, Biological and Environmental Research, Terrestrial Carbon Program (DE-FG02-04ER63917 and DE-FG02-04ER63911)), AfriFlux, AsiaFlux, CarboAfrica, CarboEuropeIP, CarboItaly, CarboMont, ChinaFlux, Fluxnet-Canada (supported by CFCAS, NSERC, BIOCAP, Environment Canada, and NRCan), GreenGrass, KoFlux, LBA, NECC, OzFlux, TCOS-Siberia, USCCC. We acknowledge the financial support to the eddy covariance data harmonization provided by CarboEuropeIP, FAO-GTOS-TCO, iLEAPS, Max Planck Institute for Biogeochemistry, National Science Foundation, University of Tuscia, Université Laval, Environment Canada and US Department of Energy and the database development and technical support from Berkeley Water Center, Lawrence Berkeley National Laboratory, Microsoft Research eScience, Oak Ridge National Laboratory, University of California–Berkeley and the University of Virginia. The authors declare no conflict of interest.

Hydrol. Earth Syst. Sci. Discuss., doi:10.5194/hess-2016-344, 2016
Manuscript under review for journal Hydrol. Earth Syst. Sci.
Published: 15 July 2016

Hydrology and Earth System Sciences
Discussions

References

Ahmad, A., Anderson, T. N., and Lie, T. T.: Hourly global solar irradiation forecasting for New Zealand, Sol. Ener., 122, 1398–1408, doi:10.1016/j.solener.2015.10.055, 2015.

Allen, R. G., Pereira, L. S., Raes, D., and Smith, M.: Crop evapotranspiration, Guidelines for computing crop water requirements, FAO Irrigation and drainage paper n. 56. 326 pp., Rome, Italy, 1998.

Anderson, R. G., Lo, M.-H., Swenson, S., Famiglietti, J. S., Tang, Q., Skaggs, T. H., Lin, Y.-H., and Wu, R.-J.: Using satellite-based estimates of evapotranspiration and groundwater changes to determine anthropogenic water fluxes in land surface models, Geosci. Model Dev., 8, 3021-3031, doi:10.5194/gmd-8-3021-2015, 2015.

Baigorria, G. A., Villegas, E. B., Trebejo, I., Carlos, J. F., and Quiroz, R.: Atmospheric transmissivity: distribution and empirical estimation around the central Andes, Int. J. Climatol., 24 (9), 1121–1136, doi: http://doi.org/10.1002/joc.1060, 2004.

Baldocchi, D.D., Falge, E., Gu, L., Olson, R., Hollinger, D., Running, S., et al.: Fluxnet: a new tool to study the temporal and spatial variability of ecosystem-scale carbon dioxide, water vapor, and energy flux densities, Bull. American Met. Soc., 82 (11), 2415–3434, 2001.

Bisht, G., Venturini, V., Islam, S., and Jiang, L.: Estimation of the net radiation using MODIS (Moderate Resolution Imaging Spectroradiometer) data for clear sky days, Remote Sens. Environ., 97 (1), 52–67, doi:10.1016/j.rse.2005.03.014, 2005.

Boulifa, M., Adane, A., Rezagui, A., and Ameur, et. Z..: Estimate of the Global Solar Radiation by Cloudy Sky Using HRV Images, Ener. Proc., 74, 1079–1089, doi:10.1016/j.egypro.2015.07.747, 2015.

Brutsaert, W., and Sugita, M.: Application of self-preservation in the diurnal evolution of the surface energy budget to determine daily evaporation, J. Geophys. Res. Atmos., 97 (D17), 18377–18382, doi: 10.1029/92JD00255, 1992.

Burden, F., and Winkler, D.: Bayesian Regularization of Neural Networks. In D. Livingstone (Ed.), Artificial Neural Networks SE - 3, 458, 23–42, Humana Press, doi:10.1007/978-1-60327-101-1_3, 2009.

Cammalleri, C., Anderson, M. C., and Kustas, W. P.: Upscaling of evapotranspiration fluxes from instantaneous to daytime scales for thermal remote sensing applications, Hydrol. Earth Sys. Sci., 18 (5), 1885–1894, doi:10.5194/hess-18-1885-2014, 2014.

Chávez, J. L., Neale, C. M. U., Prueger, J. H., and Kustas, W. P.: Daily evapotranspiration estimates from extrapolating instantaneous airborne remote sensing ET values, Irrig. Sci., 27 (1), 67–81, doi:10.1007/s00271-008-0122-3, 2008.

Chen, Z., Shi, R., and Zhang, S.: An artificial neural network approach to estimate

evapotranspiration from remote sensing and AmeriFlux data, Front. Earth Sci., 7 (1), 103–111, doi:10.1007/s11707-012-0346-7, 2013.

Colaizzi, P. D., Evett, S. R., Howell, T. A., and Tolk, J. A.: Comparison of five models to scale daily evapotranspiration from one-time-of-day measurements, Trans. ASAE, 49, 1409–1417, doi: 10.13031/2013.22056, 2006.

Crago, R. D.: Conservation and variability of the evaporative fraction during the daytime, J. Hydrol., 180 (1–4), 173–194, doi:10.1016/0022-1694(95)02903-6, 1996.

Dahmani, K., Notton, G., Voyant, C., Dizene, R., Nivet, M. L., Paoli, C., and Tamas, W.: Multilayer Perceptron approach for estimating 5-min and hourly horizontal global irradiation from exogenous meteorological data in locations without solar measurements, Ren. Ener., 90, 267–282. doi:10.1016/j.renene.2016.01.013, 2016.

Delogu, E., Boulet, G., Olioso, A., Coudert, B., et al.: Reconstruction of temporal variations of evapotranspiration using instantaneous estimates at the time of satellite overpass, Hydrol. Earth Syst. Sci., 16 (8), 2995–3010, doi:10.5194/hess-16-2995-2012, 2012.

Foken, T., Wimmer, F., Mauder, M., Thomas, C., and Liebethal, C.: Some aspects of the energy balance closure problem, Atm. Chem. Phys., 6 (12), 4395–4402, doi:10.5194/acp-6-4395-2006, 2006.

Franssen, H. J. H., Stöckli, R., Lehner, I., Rotenberg, E., and Seneviratne, S. I.: Energy balance closure of eddy-covariance data: A multisite analysis for European FLUXNET stations, Agric. For. Meteorol., 150 (12), 1553–1567, doi:10.1016/j.agrformet.2010.08.005, 2010.

Gardner, M. W., and Dorling, S. R.: Artificial neural networks (the multilayer perceptron)—a review of applications in the atmospheric sciences, Atmos. Environ., 32 (14–15), 2627–2636, doi:10.1016/S1352-2310(97)00447-0, 1998.

Gentine, P., Entekhabi, D., Chehbouni, A., Boulet, G., and Duchemin, B.: Analysis of evaporative fraction diurnal behaviour, Agric. For. Meteorol., 143 (1–2), 13–29, doi:10.1016/j.agrformet.2006.11.002, 2007.

Hasni, A., Sehli, A., Draoui, B., Bassou, A., and Amieur, B.: Estimating Global Solar Radiation Using Artificial Neural Network and Climate Data in the South-western Region of Algeria, Energy Proc., 18, 531–537, doi:10.1016/j.egypro.2012.05.064, 2012.

Hoedjes, J. C. B., Chehbouni, A., Jacob, F., Ezzahar, J., and Boulet, G.: Deriving daily evapotranspiration from remotely sensed instantaneous evaporative fraction over olive orchard in semi-arid Morocco, J. Hydrol., 354 (1–4), 53–64, doi:10.1016/j.jhydrol.2008.02.016, 2008.

Huang, G., Liu, S., and Liang, S.: Estimation of net surface shortwave radiation from MODIS data, Int. J. Remote Sens., 33 (3), 804–825, doi:10.1080/01431161.2011.577834, 2012.

Jackson, R. D., Hatfield, J. L., Reginato, R. J., Idso, S. B., and Pinter, P. J. Jr.: Estimation of

daily evapotranspiration from one time-of-day measurements, Agric. Wat. Man., 7 (1–3), 351–362, doi:10.1016/0378-3774(83)90095-1, 1983.

Khatib, T., Mohamed, A., and Sopian, K.: A review of solar energy modeling techniques, Ren. Sust. Energy Rev., 16 (5), 2864–2869, doi: 10.1016/j.rser.2012.01.064, 2012.

Laine, V., Venäläinen, A., Heikinheimo, M., and Hyvärinen, O.: Estimation of Surface Solar Global Radiation from NOAA AVHRR Data in High Latitudes, J. Appl. Meteorol., 38 (12), 1706–1719, doi: http://dx.doi.org/10.1175/1520-0450(1999)038<1706:EOSSGR>2.0.CO;2, 1999.

Lazzús, J. A., Pérez Ponce, A. A., and Marin, J.: Estimation of global solar radiation over the city of La Serena (Chile) using a neural network, Appl. Sol. Ener., 47 (1), 66–73, doi: 10.3103/S0003701X11010099, 2011.

Li, M.-F., Tang, X.-P., Wu, W., and Liu, H.-B.: General models for estimating daily global solar radiation for different solar radiation zones in mainland China, Energy Conv. Manag., 70, 139–148, doi: 10.1016/j.enconman.2013.03.004, 2013.

Mauder, M., and Foken, T.: Impact of post-field data processing on eddy covariance flux estimates and energy balance closure, Meteorolog. Zeit., 15 (6), 597-609, 2006.

McCulloch, W. S., and Pitts, W.: A logical calculus of the ideas immanent in nervous activity, The Bull. Math. Biophys., 5 (4), 115–133, doi: 10.1007/BF02478259, 1943.

Mubiru, J., and Banda, E. J. K. B.: Estimation of monthly average daily global solar irradiation using artificial neural networks, Sol. Ener., 82 (2), 181–187, doi: 10.1016/j.solener.2007.06.003, 2008.

Parlange, M. B., and Katul, G. G.: Estimation of the diurnal variation of potential evaporation from a wet bare soil surface, J. Hydrol., 132 (1-4), 71–89, doi: 10.1016/0022-1694(92)90173-S, 1992.

Polo, J., Zarzalejo, L., and Ramírez, L.: Solar Radiation Derived from Satellite Images, In V. Badescu (Ed.), Modeling Solar Radiation at the Earth's Surface SE - 18, 449–462, Springer Berlin Heidelberg, doi: 10.1007/978-3-540-77455-6_18, 2008.

Ryu, Y., Baldocchi, D. D., Black, T. A., Detto, M., et al.: On the temporal upscaling of evapotranspiration from instantaneous remote sensing measurements to 8-day mean daily-sums, Agric. For. Meteorol., 152, 212–222, doi: 10.1016/j.agrformet.2011.09.010, 2012.

Senay, G. B., Velpuri, N. M., Bohms, S., Budde, M., et al.: Drought Monitoring and Assessment: Remote Sensing and Modeling Approaches for the Famine Early Warning Systems Network, In: Hydro-Meteorological Hazards, Risks, and Disasters, 233 - 262, doi: 10.1016/B978-0-12-394846-5.00009-6, 2015.

Sepulcre-Canto, G., Vogt, J., Arboleda, A., and Antofie, T.: Assessment of the EUMETSAT LSA-SAF evapotranspiration product for drought monitoring in Europe, Int. J. Appl.

Earth Obs. Geoinf., 30, 190–202, doi: 10.1016/j.jag.2014.01.021, 2014.

Shamshirband, S., Mohammadi, K., Tong, C. W., Zamani, M., et al.: A hybrid SVM-FFA method for prediction of monthly mean global solar radiation, Theor. Appl. Climatol., 1–13, doi: 10.1007/s00704-015-1482-2, 2015.

Shuttleworth, W. J., Gurney, R. J., Hsu, A. Y., and Ormsby, J. P.: FIFE: the variation in energy partition at surface flux sites, IAHS Publ., 186, 67–74, 1989.

Tang, R., Li, Z.-L., and Sun, X.: Temporal upscaling of instantaneous evapotranspiration: An intercomparison of four methods using eddy covariance measurements and MODIS data, Remote Sens. Environ., 138, 102–118, doi: 10.1016/j.rse.2013.07.001, 2013.

Tang, R., Tang, B., Wu, H., Li, Z. L.: On the feasibility of temporally upscaling instantaneous evapotranspiration using weather forecast information, Int. J. Remote Sens., 36 (19-20), doi: 10.1080/01431161.2015.1029597, 2015.

Van Niel, T. G., McVicar, T. R., Roderick, M. L., van Dijk, A. I. J. M., et al.: Upscaling latent heat flux for thermal remote sensing studies: Comparison of alternative approaches and correction of bias, J. Hydrol., 468–469, 35–46, doi: 10.1016/j.jhydrol.2012.08.005, 2012.

Wang, S.-C.: Artificial Neural Network. In: Interdisciplinary Computing in Java Programming SE - 5, 743, 81–100, Springer US, doi: 10.1007/978-1-4615-0377-4_5, 2003.

Wilson, K., Goldstein, A., Falge, E., Aubinet, M., et al.: Energy balance closure at FLUXNET sites, Agric. For. Meteorol., 113 (1–4), 223–243, doi: 10.1016/S0168-1923(02)00109-0, 2002.

Xu, T., Liu, S., Xu, L., Chen, Y., Jia, Z., Xu, Z., & Nielson, J.: Temporal Upscaling and Reconstruction of Thermal Remotely Sensed Instantaneous Evapotranspiration, Remote Sens., 7 (3), 3400, doi: 10.3390/rs70303400, 2015.

Hydrol. Earth Syst. Sci. Discuss., doi:10.5194/hess-2016-344, 2016
Manuscript under review for journal Hydrol. Earth Syst. Sci.
Published: 15 July 2016

Hydrology and Earth System Sciences
Discussions
Open Access
EGU

Table 1: Statistical analysis of the performance of ANN in predicting R_{Sd} under varying sky conditions represented by four different classes of daily atmospheric transmissivity (τ). Here the statistical metrics of R_{Sd_pred} for two different upscaling hours (1100 and 1330 h) are presented.

Time-of-daytime (h)	τ	R^2	RMSE (MJ m^{-2} d^{-1})	IA	MAPE	Bias (MJ m^{-2} d^{-1})
1100	τ_1	0.67	1.84	0.67	53.56	1.12
	τ_2	0.79	2.45	0.80	16.69	0.59
	τ_3	0.88	2.30	0.82	9.17	-0.74
	τ_4	0.98	0.63	0.95	1.69	0.08
1330	τ_1	0.65	1.77	0.67	51.50	1.06
	τ_2	0.81	2.44	0.81	16.83	0.69
	τ_3	0.89	2.23	0.83	8.94	-0.85
	τ_4	0.98	0.89	0.95	2.40	-0.46

Hydrol. Earth Syst. Sci. Discuss., doi:10.5194/hess-2016-344, 2016
Manuscript under review for journal Hydrol. Earth Syst. Sci.
Published: 15 July 2016

Hydrology and Earth System Sciences
Discussions
Open Access
EGU

Table 2: A summary of ET_d error statistics by comparing the performance of R_S, R_STOA and EF upscaling methods with regard to different sky conditions. Here τ_1 represents low atmospheric transmissivity due to high cloudiness while τ_4 represents high transmissivity under clear sky conditions.

Time-of-daytime (h)	τ	R^2			RMSE (MJ m^{-2} d^{-1})			IA			MAPE			Bias (MJ m^{-2} d^{-1})		
		R_S	R_STOA	EF	R_S	R_STOA	EF	R_S	R_STOA	EF	R_S	R_STOA	EF	R_S	R_STOA	EF
1100	τ_1	0.49	0.32	0.32	1.34	1.65	2.07	0.72	0.67	0.71	50.14	66.70	64.19	-0.13	-0.04	0.05
	τ_2	0.72	0.70	0.69	1.73	1.81	1.93	0.81	0.78	0.69	26.47	32.41	36.42	-0.21	-0.19	-0.95
	τ_3	0.72	0.73	0.79	1.99	1.94	2.38	0.81	0.79	0.59	24.69	25.66	40.37	-0.24	-0.37	-1.78
	τ_4	0.77	0.81	0.68	1.32	1.13	2.00	0.84	0.81	0.49	32.17	30.02	55.43	0.05	-0.19	-1.34
1330	τ_1	0.52	0.34	0.29	1.21	1.68	2.34	0.73	0.69	0.71	48.29	66.09	68.14	-0.11	0.08	0.12
	τ_2	0.73	0.72	0.71	1.71	1.93	1.86	0.82	0.79	0.71	26.12	33.71	35.33	-0.01	0.24	-0.88
	τ_3	0.75	0.75	0.76	1.89	1.96	2.43	0.82	0.82	0.61	23.17	25.82	41.65	0.09	0.14	-1.75
	τ_4	0.79	0.86	0.80	1.32	1.09	1.86	0.84	0.86	0.49	29.54	26.59	53.91	0.10	0.11	-1.38

Hydrol. Earth Syst. Sci. Discuss., doi:10.5194/hess-2016-344, 2016
Manuscript under review for journal Hydrol. Earth Syst. Sci.
Published: 15 July 2016

Hydrology and Earth System Sciences
Discussions
Open Access
EGU

Table 3: Error statistics of ET_{d_pred} at four different temporal scales from three ET_i upscaling methods.

Time-of-daytime (h)	Temporal scale	R^2			RMSE (MJ m^{-2} d^{-1})			IA			MAPE			Bias (MJ m^{-2} d^{-1})		
		R_S	R_STOA	EF	R_S	R_STOA	EF	R_S	R_STOA	EF	R_S	R_STOA	EF	R_S	R_STOA	EF
1100	Daily	0.71	0.72	0.71	1.79	1.85	2.16	0.82	0.80	0.67	28.80	32.98	57.00	0.19	0.22	1.21
	8-days	0.86	0.84	0.85	1.17	1.22	1.65	0.87	0.86	0.67	18.50	20.63	46.96	0.19	0.22	1.16
	Monthly	0.89	0.88	0.88	0.99	1.04	1.61	0.89	0.67	0.67	15.52	17.22	49.72	0.19	0.22	1.16
	Annually	0.92	0.91	0.93	0.57	0.62	1.33	0.87	0.84	0.54	11.12	12.54	45.88	0.19	0.22	1.21
1330	Daily	0.75	0.74	0.69	1.74	1.89	2.2	0.83	0.82	0.67	26.59	29.89	56.45	-0.04	0.17	-1.18
	8-days	0.87	0.86	0.84	1.11	1.21	1.7	0.88	0.88	0.68	16.80	17.97	50.36	-0.04	0.17	-1.18
	Monthly	0.90	0.90	0.87	0.93	1.00	1.59	0.90	0.89	0.68	13.69	14.85	48.08	-0.04	0.17	-1.18
	Annually	0.93	0.93	0.92	0.51	0.53	1.31	0.88	0.88	0.54	9.00	9.70	44.13	-0.04	0.17	-1.18

Hydrol. Earth Syst. Sci. Discuss., doi:10.5194/hess-2016-344, 2016
Manuscript under review for journal Hydrol. Earth Syst. Sci.
Published: 15 July 2016

1

Figure 1. A conceptual diagram of the methodology. On the left side is a representation of predicting daily incoming short wave radiation (R_{Sd_pred}). The ANN is trained to learn the system response to a combination of explanatory variables i.e. instantaneous incoming short wave radiation (R_{Si}), instantaneous exo-atmospheric shortwave radiation ($R_{Si}TOA$), daily exo-atmospheric shortwave radiation ($R_{Sd}TOA$), solar zenith angle (θ_Z), and day length (L_D), by being fed with a sample data of observed daily incoming short wave radiation (R_{Sd}) which is the dependant variable. On the right side are methods of upscaling instantaneous (ET_i) to daily ET (ET_d) using our R_S method (a) and other two approaches (b, c) are the R_{STOA} and EF methods respectively used which are used for comparison.

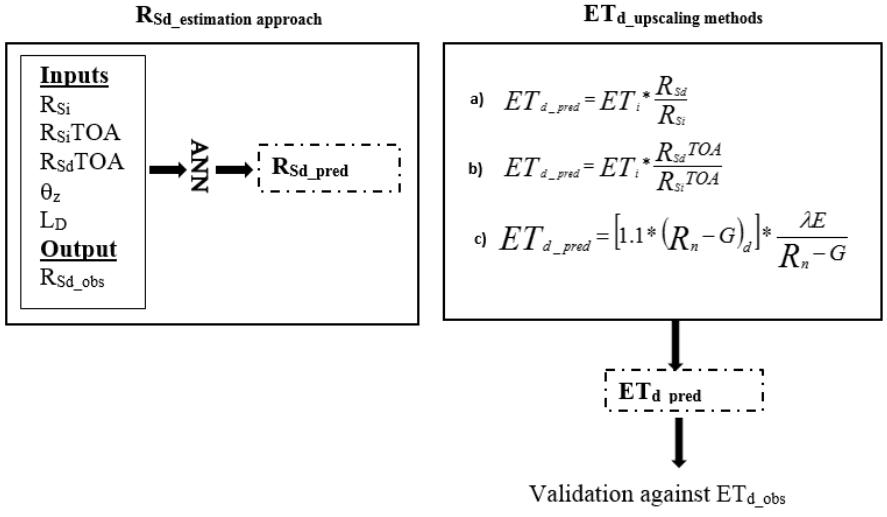

2

3

Figure 2. Schematic representation of a simple artificial network model. The artificial neuron has five input variables, for the intended output. These inputs are then assigned weights (*W)* and bias (b), and the sum of all these products ($\sum$) is fed to an activation function (f). The activation function alters the signal accordingly and passes the signal to the next neuron(s) until the output of the model is reached (Mathworks, 2015).

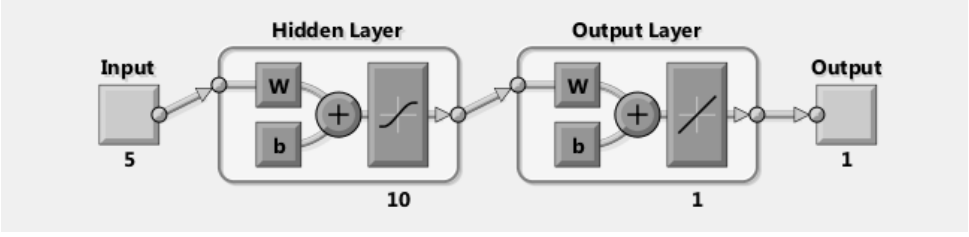

4

Hydrol. Earth Syst. Sci. Discuss., doi:10.5194/hess-2016-344, 2016
Manuscript under review for journal Hydrol. Earth Syst. Sci.
Published: 15 July 2016

Hydrology and Earth System Sciences
Discussions

1

Figure 3. Distribution of 126 sites of the FLUXNET eddy covariance network used in the present study with 85 and 41 sites for training and validation, respectively between the years 1999 and 2006.

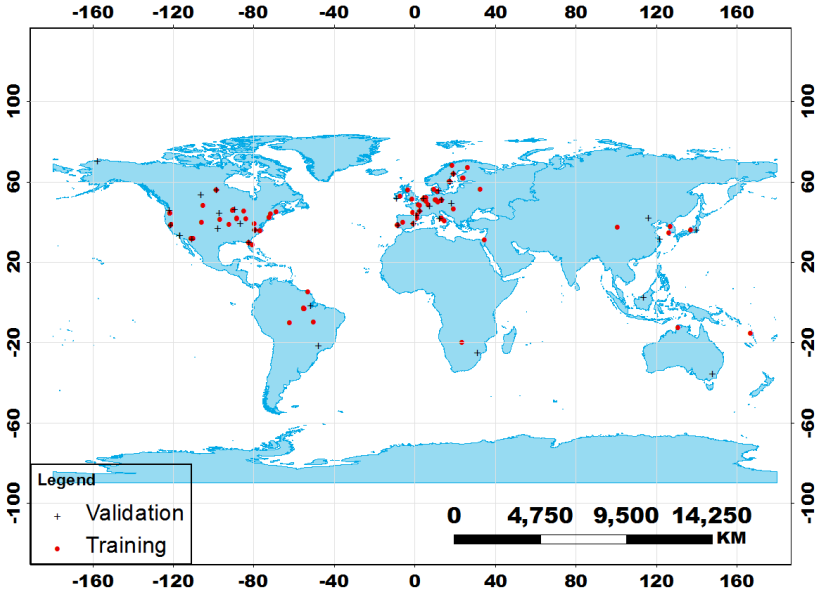

2
3
4
5
6
7
8
9
10
11
12
13
14
15

Hydrol. Earth Syst. Sci. Discuss., doi:10.5194/hess-2016-344, 2016
Manuscript under review for journal Hydrol. Earth Syst. Sci.
Published: 15 July 2016

Figure 4. Statistical metric of R_{Sd_pred} by ANN for different time-of-daytime. As the study is intended for remote sensing application, we demonstrate the potential of the method for future research in the case where satellite will be used and as such we pick MODIS overpass time as an example to highlight on the predictive ability of the ANN at the specific overpass times.

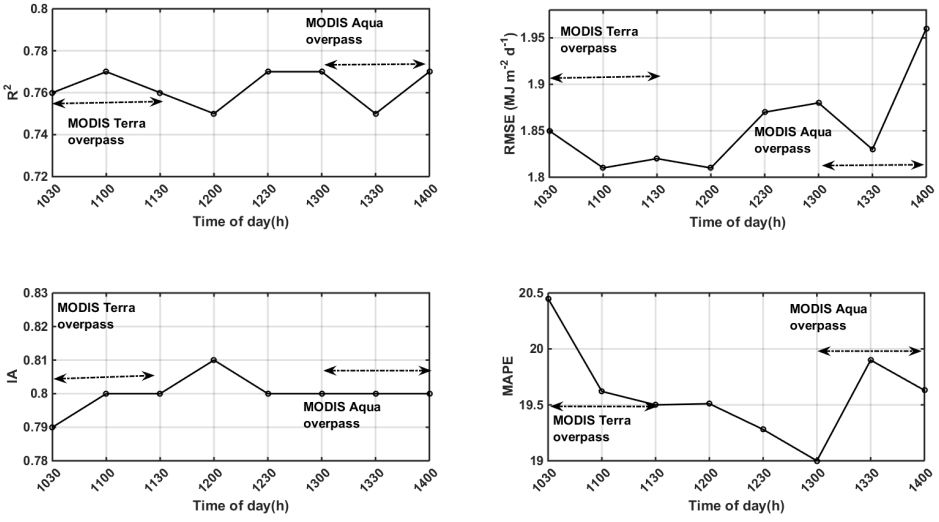

Hydrol. Earth Syst. Sci. Discuss., doi:10.5194/hess-2016-344, 2016
Manuscript under review for journal Hydrol. Earth Syst. Sci.
Published: 15 July 2016

1

Figure 5. Scatter plots between R_{Sd_pred} versus R_{Sd_obs} for different levels of daily atmospheric transmissivity classes (τ) from (a) 1100 and (b) 1330 hours upscaling. Here τ_1–τ_4 represent daily atmospheric transmissivity of four different class, 0.25≥τ≥0, 2 0.5≥τ≥0.25, 0.75≥τ≥0.5, and 1≥τ≥0.75, respectively, with τ_1 signifying high degree of cloudiness (or overcast skies) whereas τ_4 indicates clear skies.

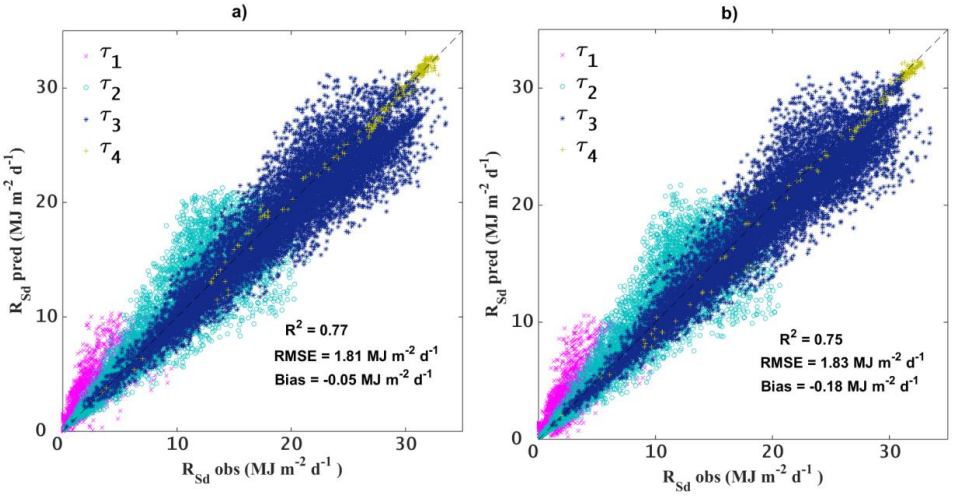

2
3
4
5
6
7
8
9
10
11
12
13
14
15

Hydrol. Earth Syst. Sci. Discuss., doi:10.5194/hess-2016-344, 2016
Manuscript under review for journal Hydrol. Earth Syst. Sci.
Published: 15 July 2016

Hydrology and Earth System Sciences
Discussions
Open Access
EGU

1

Figure 6. Statistical summary of ET_{d_pred} for different time-of-daytime using Eq. (1) based on R_{Si} and R_{Sd_pred}. As the study is intended for remote sensing application, we once again demonstrate the potential of the method for future research in the case where satellite will be used and as such we pick MODIS Terra-Aqua overpass time.

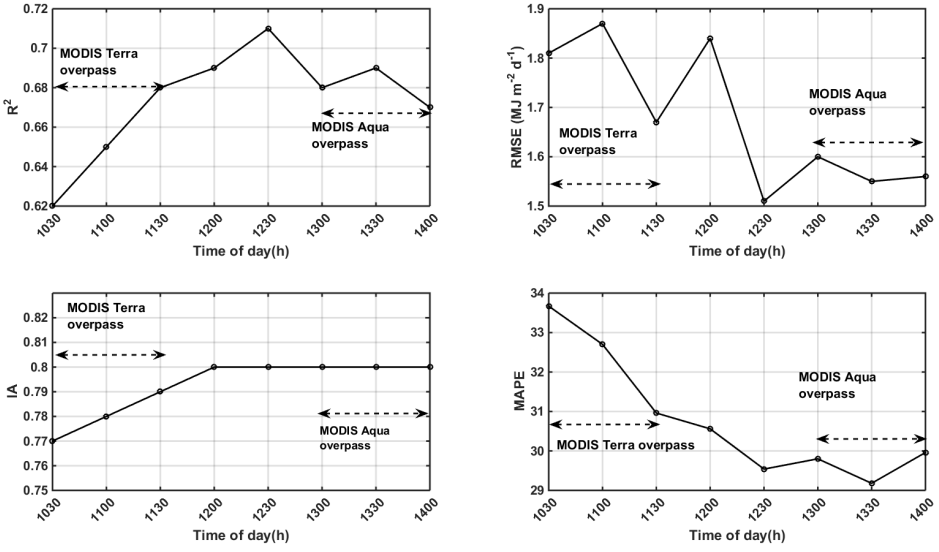

2
3
4
5
6
7
8
9
10
11
12
13
14

Hydrol. Earth Syst. Sci. Discuss., doi:10.5194/hess-2016-344, 2016
Manuscript under review for journal Hydrol. Earth Syst. Sci.
Published: 15 July 2016

Hydrology and Earth System Sciences
Discussions
Open Access
EGU

1

Figure 7. ET_{d_pred} obtained through eq. (1) versus ET_{d_obs} for different levels of τ from both forenoon and afternoon upscaling (1100 and 1300 daytime hours).

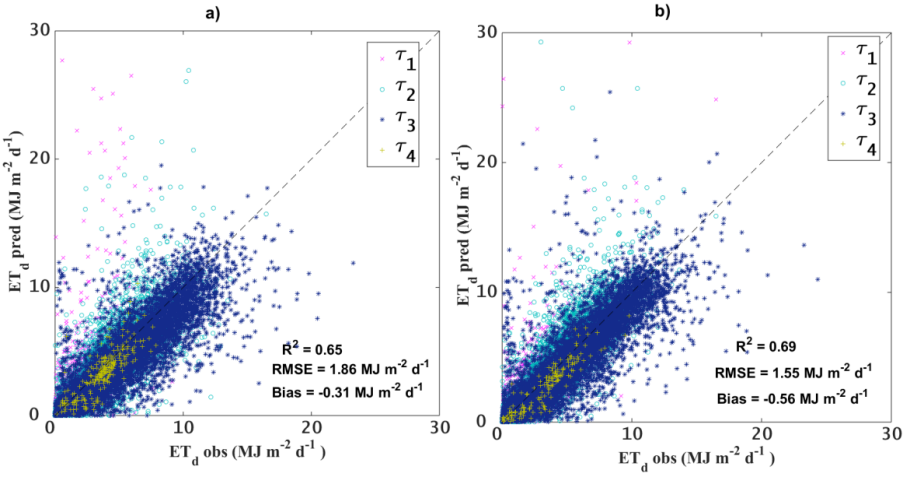

2
3
4
5
6
7
8
9
10
11
12
13
14
15
16
17

Hydrol. Earth Syst. Sci. Discuss., doi:10.5194/hess-2016-344, 2016
Manuscript under review for journal Hydrol. Earth Syst. Sci.
Published: 15 July 2016

Figure 8. Assessing the statistical metrics of ET_{d_pred} (using eq.1) for different levels of daily atmospheric transmissivity classes (representing cloudy to clear skies) for both 1100h and 1330h time-of-daytime ET_i scaling.

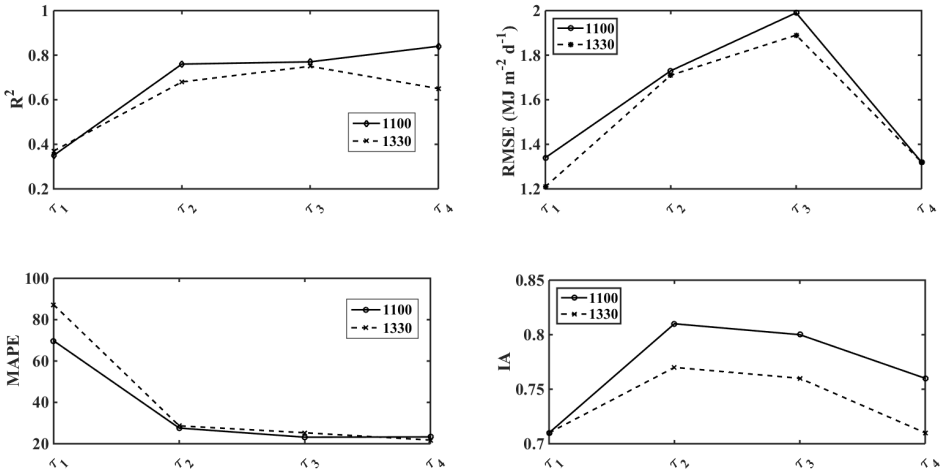

Hydrol. Earth Syst. Sci. Discuss., doi:10.5194/hess-2016-344, 2016
Manuscript under review for journal Hydrol. Earth Syst. Sci.
Published: 15 July 2016

Hydrology and Earth System Sciences
Discussions

1

Figure 9. Biome specific error characteristics of ET_{d_pred} displaying the box plots of (a) RMSE and (b) coefficient of determination (R^2). The biome classes are evergreen broadleaf forest (EBF), evergreen needleleaf forest (ENF), deciduous broadleaf forest (DBF), shrubland (SH), cropland (CRO), and grassland (GRA), respectively.

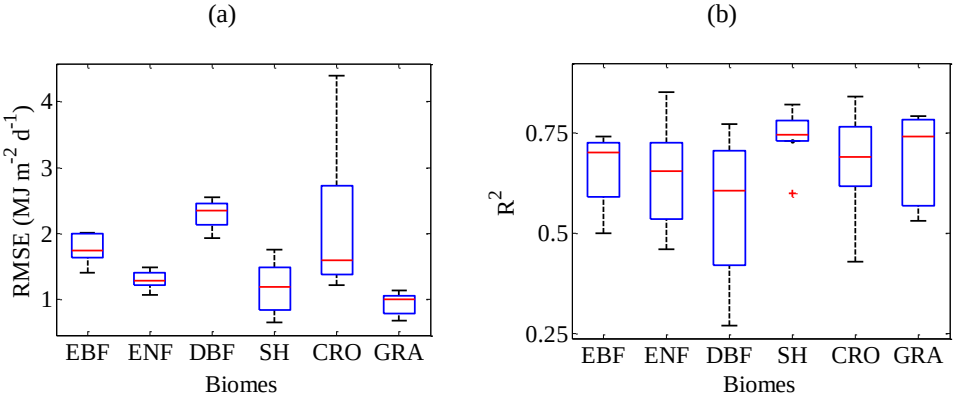

2
3
4

Figure 10. Time series comparison between measured and predicted ET_d for four representative sites located in Australia, Brazil, South Africa and Sweden.

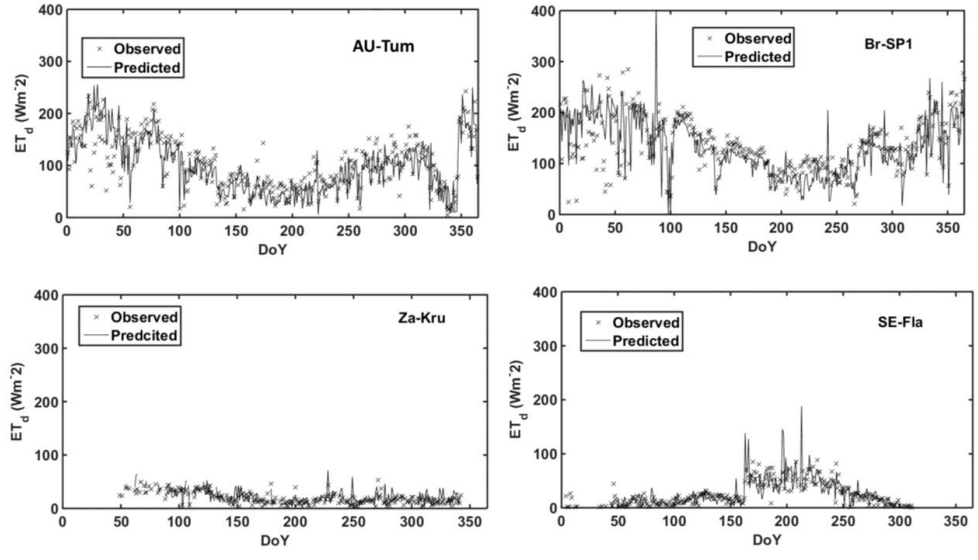

5

Hydrol. Earth Syst. Sci. Discuss., doi:10.5194/hess-2016-344, 2016
Manuscript under review for journal Hydrol. Earth Syst. Sci.
Published: 15 July 2016

1

Figure 11. Statistical metrics of ET_{d_pred} from three different ET_i upscaling approaches [shortwave incoming radiation (R_S), exo-atmospheric shortwave radiation (R_STOA) and evaporative fraction (EF)] at different temporal scales based on ETi measurements at (a) 1100h and (b) 1330h time-of-daytime.

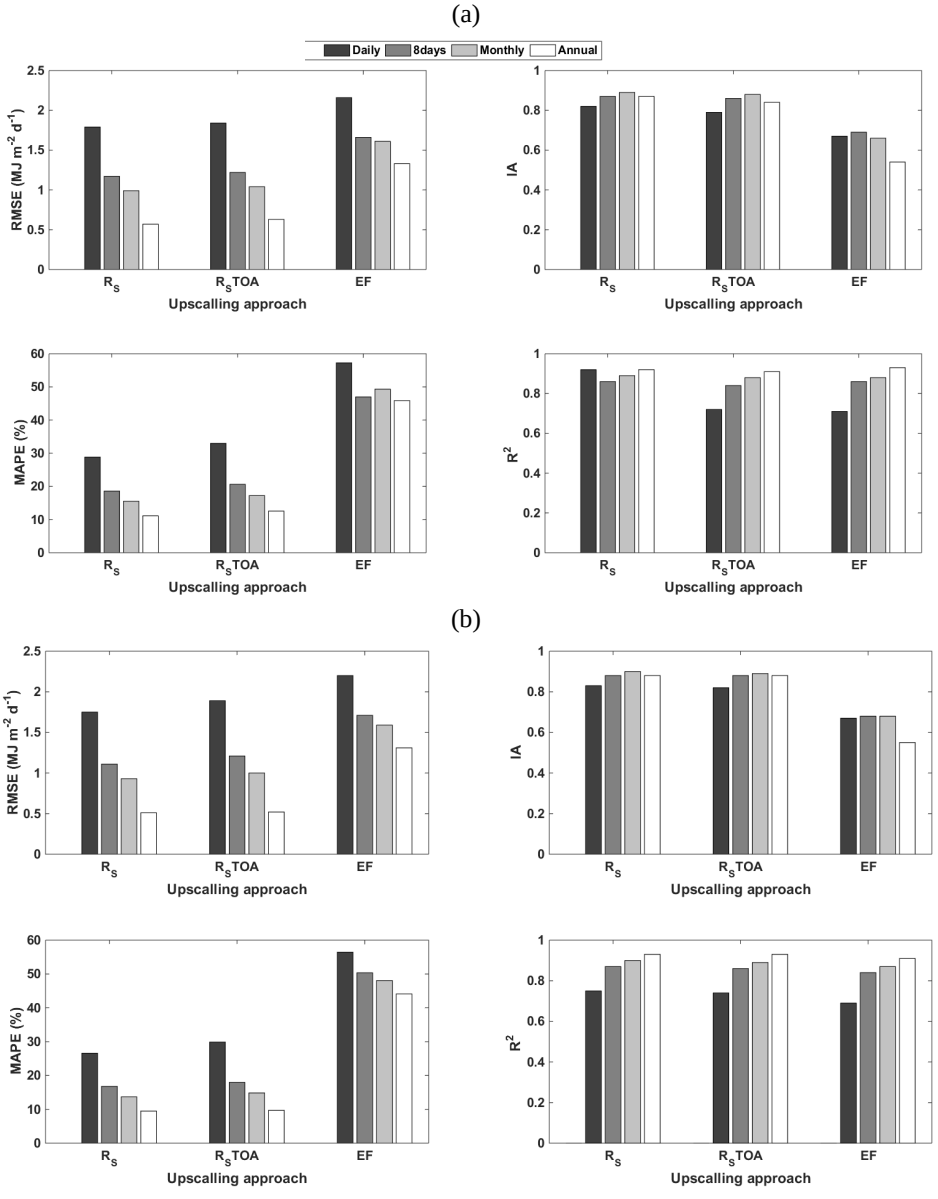

2